

XIX INTERNATIONAL SYMPOSIUM ON LEPTON AND PHOTON INTERACTION  
AT HIGH ENERGY  
Stanford University, August 9-14, 1999

L.G.Landsberg  
State Research Center, Institute for High Energy Physics,  
Protvino, Moscow region, Russia, 142284

**STUDY OF THE PRIMAKOFF REACTIONS  
AT HIGH ENERGY**

arXiv:hep-ex/9908034v1 6 Aug 1999

## Abstract

In this talk the Coulomb production reactions at high energy are discussed as well as the study of electromagnetic properties of hadrons (mesons and hyperons) in these processes. The results of previous investigations are summed together with some recent data of SELEX(Fermilab) and SPHINX(IHEP) experiments.

## 1 Introduction

Investigation of electromagnetic hadron decays plays an important role in elementary-particle physics. These processes, governed by the interaction of real and virtual photons with the electric charges of quark fields, make it possible to obtain unique information on the character of various quark configurations in hadrons, the mechanism of mixing, the electromagnetic structure of strongly interacting particles, and on some phenomenological features of such particles (magnetic moments, formfactors, polarizability, etc.). Recent years have seen a significant progress in this field.

Radiative hadron decays of the type  $a \rightarrow h + \gamma$  can be studied by both direct and indirect methods. In the former case, particle  $a$  is produced in a reaction and its decay  $a \rightarrow h + \gamma$  is detected directly in the experimental setup. Among indirect methods one should mention the process of interaction of primary particle  $h$  with a virtual photon in the Coulomb field of the nucleus

$$h + (Z, A) \rightarrow a + (Z, A) \quad (1)$$

As we will show later, at a very high energy  $E_h$  Coulomb reaction (1) is characterized by small values of the squared 4-momentum transfer  $q^2$  which is identical with the squared 4-momentum  $q^2$  of the virtual photon propagator. Thus, at  $q^2 \simeq 0$  the virtual photons are quasi-real. In this approximation the cross section for this Coulomb production process is proportional to the radiative width  $\Gamma(a \rightarrow h + \gamma)$ .

The main aim of my talk is to discuss these electromagnetic Coulomb processes and their application to the study of radiative decays of hadrons and to the search for some exotic states. Actually, the type (1) reactions involving collisions with virtual (quasireal) photons are photoproduction reactions on primary hadrons  $h$ . With pion, kaon, or hyperon beams we have unique possibility to study photoproduction on unstable "targets" ( $\pi$ ,  $K$ ,  $Y$ ). The Coulomb production mechanism was considered for the first time independently by H.Primakoff [1] and by I. Pomeranchuk and I. Schmushkevich [2]. It is often designated as the Primakoff production or Primakoff reaction.

## 2 Direct Methods of Studying the Radiative Decays of Hadrons

In this type of experiments the particles under study ( $a$ ) are produced either in hadron reactions or in electromagnetic interactions (photoproduction; resonance production in  $e^+e^-$  collisions). As a rule, to select rare electromagnetic decays

$$a \rightarrow h + \gamma, \quad (2)$$

$$a \rightarrow b_1 + b_2 + \gamma, \quad (3)$$

it is necessary to detect all the decay products — charge particles as well as photons — to measure their momenta and energy and to reconstruct the effective mass of decay particles ( $M(h\gamma)$ ;  $M(b_1b_2\gamma)$ ).

In the directly detected  $a \rightarrow h + \gamma$  decays or more intricate electromagnetic processes, we must suppress a background from the decay  $\pi^0 \rightarrow \gamma\gamma$  with one photon being lost. A similar situation prevails, for example, in searches for the decay  $\omega \rightarrow \pi^+\pi^-\gamma$  against the background from the main decay mode  $\omega \rightarrow \pi^+\pi^-\pi^0$ ,  $\pi^0 \rightarrow \gamma(\gamma)$  [hereafter,  $(\gamma)$  stands for the lost photon]. Reliable separation of rare radiative decays involving single photons requires a complete detection of all secondaries (both charged and neutral ones), measurement of their momenta, and reconstruction of effective masses with the highest possible resolution. The background from the lost photons can be minimized by equipping the setup with a veto system consisting of counters with a low threshold for photon detection and having the maximum possible coverage. This system also includes a hodoscopic  $\gamma$  spectrometer detecting photons from radiative decays in the operating acceptance of the setup. A strong kinematical constraint on the processes in question can also play an important role. The point is that the background from the events with a lost photon does not yield a narrow peak at the mass of a particle under study and can therefore be considerably reduced owing to kinematical constraints. The above is illustrated by searches for the radiative decay  $\omega \rightarrow \pi^+\pi^-\gamma$  in the experiments with the Lepton-F [3] and ASTERIX [4] setups. The background from the lost photons was substantially suppressed by appropriately chosen conditions and using a veto system in the former case and by imposing more stringent kinematical constraints in the latter case. As a result, the two experiments yield approximately the same upper limit on the probability of the above radiative decay:  $BR(\omega \rightarrow \pi^+\pi^-\gamma) < 4 \times 10^{-3}$  (at a 95% C.L.) This demonstrates that radiative decays can be sought directly even if their probabilities are less than 1% of the probabilities of the most dangerous background processes. At the same time, the decay  $\omega \rightarrow \pi^0\pi^0\gamma$ , for which the background conditions proved to be much more favorable (the process  $\omega \rightarrow 3\pi^0$ , which could mimic the decay  $\omega \rightarrow \pi^0\pi^0\gamma$  because of the lost photon, is forbidden by  $P$  and  $C$  conservation in strong and electromagnetic interactions), was recorded at a significantly lower level of  $BR(\omega \rightarrow \pi^0\pi^0\gamma) = (7.2 \pm 2.6) \times 10^{-5}$  [5]. The same is true for several other electromagnetic decays with a relatively small background. The results of several experiments for the direct study of rare radiative decays of mesons are presented in Table 1 and in [3-10]. An overview of various methods for detecting electromagnetic decays is given, for example, in review papers [11-14].

### 3 Coulomb production of hadrons and the study of their radiative decays

To determine the radiative widths of some excited hadrons for which direct measurements involve considerable difficulties or are impossible, it was proposed long ago to use coherent electromagnetic production of particles in the Coulomb field of heavy nuclei ([1,2]), see also [15-18]). In the small-width approximation as applied to the resonance state  $a$  in (1), the cross section for electromagnetic production has the form

$$\begin{aligned} & \left[ \frac{d\sigma[h + (Z, A) \rightarrow a + (Z, A)]}{dq^2} \right]_{\text{Coul}} = \\ & = |T_{\text{Coul}}|^2 = 8\pi\alpha Z^2 \cdot \frac{2J_a + 1}{2J_h + 1} \cdot \Gamma(a \rightarrow h\gamma) \\ & \times \left[ \frac{(q^2 - q_{\text{min}}^2)}{q^4} \right] \cdot \left( \frac{M_a}{(M_a^2 - M_h^2)^3} \right)^3 \cdot |F_Z(q^2)|^2, \end{aligned} \quad (4)$$

where  $Z$  is the charge of the nucleus;  $\alpha$  is the fine-structure constant;  $\Gamma(a \rightarrow h\gamma)$  is the radiative decay width of particle  $a$ ;  $J_a$  and  $J_h$  are the spins of particles  $a$  and  $h$ , respectively;  $M_a$  and  $M_h$  are their masses;  $F_Z(q^2)$  is the nuclear electromagnetic form factor;  $q_{\min}^2 = (M_a^2 - M_h^2)^2/4E_h^2$  is the minimum 4-momentum transfer squared; and  $E_h$  is the energy of the primary particle  $h$ . If photons appear as primary particles, an additional factor of two must be included in the expression for the differential cross section.

As it is seen from (4) the Coulomb cross section increases fast with decreasing  $q^2$ . It can easily be found that the cross section  $[d\sigma/dq^2]_{\text{Coul}}$  attains a maximum at  $q_0^2 = 2q_{\min}^2$  and that  $[d\sigma/dq^2]_{\text{Coul}}^{\max} \propto q_{\min}^{-2} \propto E_h^2$ . As the primary momentum increases, the cross-section value at the maximum increases in proportion to  $E_h^2$ , whereas the position of this maximum shifts toward lower values of  $q^2$ . The total cross section for the Coulomb process increases as  $\ln E_h$ . Concurrently, the differential cross section for a coherent process that is governed by a strong interaction exhibits a much broader distribution in  $q^2$ , and the region of small  $q^2$  is dominated by the Coulomb contribution. The total Coulomb production cross section has the form

$$\begin{aligned} \sigma[h + (Z, A) \rightarrow a + (Z, A)]_{\text{Coul}} &= \\ &= \frac{2J_a + 1}{2J_h + 1} \cdot 8\pi\alpha Z^2 \Gamma(a \rightarrow h\gamma) \left( \frac{M_a}{M_a^2 - M_h^2} \right)^3 \times \\ &\times \int_{q_{\min}^2}^{q_{\max}^2} \frac{(q^2 - q_{\min}^2)}{q^4} |F_Z(q^2)|^2 d(q^2) = \sigma_0 \cdot \Gamma(a \rightarrow h\gamma). \end{aligned} \quad (5)$$

The quantity  $q_{\max}^2$  bounds the integration domain dominated by Coulomb processes. Certainly, a more precise expression for  $\sigma_0$  can be obtained and used in the data analysis, in which  $a \rightarrow h\gamma$  decay is expressed more carefully, in a relativistic Breit-Wigner resonance form.

The coherent production of hadrons by a primary particle  $h$  on nuclei  $(Z, A)$  is a rather complicated process affected by both electromagnetic and strong interactions. The contribution of strong interactions leads to a broader distribution in momentum transfer squared  $q^2$ . The differential cross section for coherent particle production on nuclei can be represented as

$$[d\sigma/dq^2]_{\text{Coherent}} = |T_{\text{Coul.}} + e^{i\varphi} T_{\text{strong}}|^2, \quad (6)$$

where  $T_{\text{Coul.}}$  is the amplitude of Coulomb production,  $T_{\text{strong}}$  is the amplitude of a coherent process that is governed by a strong interaction, and  $\varphi$  is the relative phase of the two amplitudes. For the understanding of a possibility to separate these coherent processes it is instructive to formulate their main characteristics which is done in Table 2.

It can be seen from Table 2 that in accordance with quantum numbers of the produced hadrons in (1) two possible scenarios for the strong coherent background can take place:

- A. Coherent diffractive background is forbidden by selection rules for (1) and the leading coherent background is determined usually by  $\omega$  reggeon exchange in  $t$  channel of the reaction. This amplitude dies at a very high energy. In several cases this background is also reduced in the region of small  $q^2$  (as  $\propto q^2 - q_{\min}^2$ ). The absence of diffractive coherent background significantly simplifies the separation of the Coulomb process.
- B. Coherent diffractive background plays a leading role in reaction (1). In this case the separation of the Coulomb process is much more difficult and might be performed only in the region of very small  $q^2 (< 10^{-3} \text{ GeV}^2)$  and with a very large statistics.

Let us complete the discussion of the Coulomb production reactions making several conclusions:

1. The Coulomb production reactions open a new possibility to study rare radiative decays  $a \rightarrow h + \gamma$  if these processes cannot be detected directly due to the background from the decay  $a \rightarrow h + \pi^0$ ;  $\pi^0 \rightarrow \gamma + (\gamma)$  with lost photons or if the decay width is too small for a direct measurement (the later case takes place, for example, for  $\Sigma^0 \rightarrow \Lambda + \gamma$  decays).
2. The Coulomb production processes open a unique possibility to study the photoproduction reactions on unstable “targets” (like pions, kaons, hyperons), which can be very important for the search for exotic hadrons, for studying some electromagnetic properties of unstable hadrons (their polarizability, for example) and other phenomena.
3. To accomplish this study it is necessary to separate the Coulomb production processes and to make the absolute measurements of their cross sections. All these require very precise and sophisticated experiments in the high energy region. This is the reason for a relatively small amount of the Coulomb production experiments which have been carried out in a 50 year period of time since the first theoretical work of H.Primakoff [1]. The main experimental results in this field at the high energies [19–31] are summarized in Table 3.

## 4 Study of the Coulomb production processes in the SELEX experiment at $E_h = 600$ GeV

In 1998 the first preliminary results of studying several Coulomb production reactions in the SELEX experiment at the Tevatron of Fermilab were obtained and are presented here in short (for more details see [32,33]).

The SELEX setup [34,35], that is used in these measurements includes the three-stage magnetic spectrometer with proportional and drift chambers, vertex microstrip detector, trigger hodoscopes, some additional microstrip detectors, RICH and TRD detectors for particle identification, three photon lead glass multichannel spectrometers, neutron calorimeter. The main measurements in the SELEX (E781) experiment were performed with a negative-charged beam of 600 GeV momentum and with practically equal amount of  $\pi^-$ -mesons and  $\Sigma^-$ -hyperons (they were identified with the beam TRD detector). The wide research program is performed by SELEX(E781) international collaboration (with the participation of scientists from Brasil, China, Germany, Israel, Italy, Mexico, Russia, United Kingdom, USA). The main part of this program involves the study of charmed and strange-charmed baryons, the search for exotic states, the investigation of electromagnetic properties of hadrons and the Coulomb production processes, some other researches. A short summary of the preliminary Coulomb production results in the SELEX experiment is presented below.

### 4.1 Study of the reaction $\pi^- + (A, Z) \rightarrow [\pi^- \pi^- \pi^+] + (A, Z)$ and measurement of the radiative width for $a_2(1320)$ meson

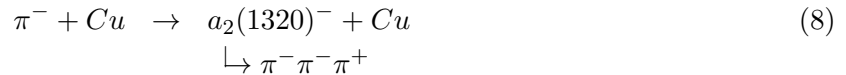
The coherent reactions

$$\pi^- + (Z, A) \rightarrow [\pi^- \pi^- \pi^+] + (A, Z) \quad (7)$$

on carbon, copper and lead nuclei were separated in the analysis of the events with 3 charge particles in the final state in the interactions of identified primary  $\pi^-$ -mesons in one of the targets. These events must satisfy the “elastic conditions” — the difference between the beam particle momentum and the sum of momenta of three secondary particles must be less than 17.5 GeV. The statistics of the selected events of (7) is tabulated in Table 4.

The  $P_T^2$  distribution<sup>1</sup> of the  $(3\pi)^-$ -system in reaction (7) for the copper target is shown, as an example, in Fig.1a. This  $dN/dP_T^2$  distribution was fitted by the sum of two exponents  $dN/dP_T^2 = C_1 \exp(-b_1 P_T^2) + C_2 \exp(-b_2 P_T^2)$  with the slopes  $b_1 = 1577 \pm 88 \text{ GeV}^{-2}$  and  $b_2 = 189.4 \pm 0.6 \text{ GeV}^{-2}$ . The second slope  $b_2$  is in a good agreement with the slope for diffractive production coherent process (7) obtained from the data [36] at  $E_\pi = 200 \text{ GeV}$ . The slope  $b_1$  corresponds to the Monte Carlo estimations for the Coulomb mechanism (with account for the  $P_T^2$  resolution).

Two  $P_T^2$  regions were defined for  $dN/dP_T^2$  distribution (see Fig.1a). In the first region ( $P_T^2 < 0.001 \text{ GeV}^2$ ) the Coulomb production process dominating. The second region ( $0.0015 < P_T^2 < 0.0035 \text{ GeV}^2$ ) was used to estimate the coherent diffractive background. The mass spectra  $M(3\pi)$  for these two regions are presented in Fig.1b. The result of diffractive background subtraction (after a proper normalization) is presented in Fig.1c. In this subtracted mass spectrum the Coulomb production of  $a_2(1320)^-$  meson in the reaction



is clearly seen. The same results were also obtained from the measurements with carbon and lead targets. After the absolute normalization of cross sections for the Primakoff reactions  $\sigma_{\text{Coulomb}}[a_2(1320)^-] = \sigma_0 \cdot \Gamma[a_2(1320)^- \rightarrow \pi^- \gamma]$ , the values for radiative width  $\Gamma[a_2(1320)^- \rightarrow \pi^- \gamma]$  from all these measurements were obtained (see Table 4). For the absolute normalization the cross sections of diffractive production reactions (7) for  $A = Pb; Cu; C$  from [36] were used.

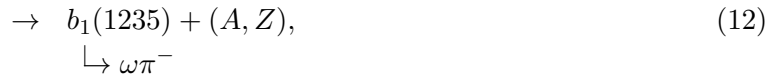
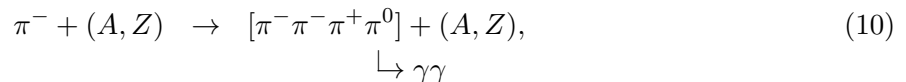
The data for the radiative width in the measurements with different targets are consistent with each other, which confirms the Coulomb production of  $a_2(1320)$  meson. The average value of radiative width over all the targets is

$$\Gamma[a_2(1320)^- \rightarrow \pi^- \gamma] = 233 \pm 31(\text{stat.}) \pm 47(\text{syst.}) \text{ KeV}. \quad (9)$$

The main source for the systematic uncertainty is the absolute normalization procedure. This value of the radiative width is preliminary and might be obtained with a better accuracy in the future. The comparison of value (10) with previous measurement [21] and with theoretical predictions [37, 38] is also presented in Table 4.

## 4.2 Further Primakoff reaction data from the SELEX experiment

### 4.2.1 Study of the coherent reactions




---

<sup>1</sup>Here  $q^2 \simeq q_{\text{min}}^2 + P_T^2 \simeq P_T^2$  at a very high momentum.

were performed at  $E_{\pi^-} = 600$  GeV on the lead, copper and carbon targets in the SELEX experiment. The Coulomb production of  $b_1(1235)^- \rightarrow \omega\pi^-$  and  $a_2(1320)^- \rightarrow \eta\pi^-$  was observed quite clearly in (12) and (14) under very favorable background conditions. The Coherent strong interaction background here is dominated by  $\omega$  exchange and is small in the region of  $P_T^2 < 0.003$  GeV<sup>2</sup>. Now the data from these Primakoff reactions are in the course of analysis to obtain the absolute normalization of their cross sections and to determine the radiative widths  $\Gamma[b_1(1235)^- \rightarrow \pi^- + \gamma]$  and  $\Gamma[a_2(1320)^- \rightarrow \pi^- + \gamma]$ .

#### 4.2.2 Study of the Coulomb production reaction

$$\Sigma^- + Pb \rightarrow \Sigma^*(1385)^- + Pb. \quad (15)$$

This Primakoff process is determined by a very small width of SU(3) forbidden radiative decay

$$\Sigma^*(1385)^- \rightarrow \Sigma^- + \gamma. \quad (16)$$

Only a short dedicated run at the SELEX facility can be used for the study of Primakoff reaction (15). The preliminary value for the upper limit of radiative width for decay (16) is obtained in this measurement

$$\Gamma[\Sigma^*(1385)^- \rightarrow \Sigma^- + \gamma] < 7\text{KeV} \quad (95\text{c.l.}) \quad (17)$$

The theoretical expectations for this width are in the region of 1– 10 KeV (see reviews [39,40] and the references herein). For comparison, the expected value of radiative width for the SU(3) allowed decay

$$\Sigma^*(1385)^+ \rightarrow \Sigma^+ + \gamma \quad (18)$$

is predicted at a level of 100 keV.

## 5 Coulomb reactions and the search for exotics

The Coulomb production processes (“Primakoff reactions”) can be of great concern not only in the study of radiative hadronic decays, but in the search for new types of hadrons as well. In the last decade the problem of existence of a novel form of hadronic matter — exotic hadrons — has become the leading direction in hadron spectroscopy. A rapid development of this field led to a significant advance in the systematics of “ordinary” hadrons (with the valence quark structure  $q\bar{q}$  or  $qqq$ ) and to the observation of several unusual states which do not fit this simplest systematics. These anomalous states are real candidates for exotic hadrons with a complicated valence internal structure (multi-quark formations  $qq\bar{q}\bar{q}$ ,  $qqq\bar{q}\bar{q}$ ; hybrid states with valence quarks and gluons  $q\bar{q}g$ ,  $qqqg$ ; pure gluonic mesons — glueballs  $gg$ ,  $ggg$ ).

The success of experiments aimed at the search for exotic hadrons and first of all for cryptoexotic states with usual quantum numbers but with anomalous dynamical properties (“hidden exotics”) is, to a great extent, determined by the appropriate choice of the production processes for which some qualitative considerations can predict more distinct manifestations of exotic states. For example, it was emphasized in a number of studies that gluon-rich diffractive production reactions on nucleons or nuclei (coherent reactions) offer some favorable grounds for exotic hadron production [41–44]. It was also stated that for some cases the electromagnetic mechanisms can be very promising for these aims [45–47].

Let us consider, for example, the exotic hadrons with hidden strangeness —  $q\bar{q}s\bar{s}$  mesons or  $qqqs\bar{s}$  baryons (here  $q = u$ - or  $d$ -quarks). Due to a significant coupling of photon with  $s\bar{s}$  pairs

through  $\phi$  meson in the framework of VDM, electromagnetic interactions can provide a natural way to embed the  $s\bar{s}$  pair into an intermediate hadron state and to produce the exotic hadron with hidden strangeness. This possibility can be realized in the resonance  $s$ -channel reaction

$$\gamma + N \rightarrow |qqqs\bar{s}\rangle \rightarrow YK \quad (19)$$

or in the Coulomb production reaction

$$h + (Z, A) \rightarrow |qqqs\bar{s}\rangle + (Z, A) \quad (20)$$

As has been shown in Section 3, the Coulomb production mechanism plays the leading role in the region of very small transfer momenta, where it is dominating over the strong interaction process. Thus, the coherent reactions at a very small  $P_T^2 (\lesssim 0.01 \text{ GeV}^2)$  can be used in the search for exotic states with hidden strangeness.

As was stated before, the most interesting Coulomb production processes were those initiated by unstable primary particles ( $\pi$ -mesons,  $K$ -mesons, hyperons), because these processes give the only possibility to study the photoproduction reactions on unstable targets. Reaction (20) for protons ( $h \equiv p$ ) is, in principle, the same as photoproduction process (19) which can be studied in a very detailed way on photon beams of electron accelerators. But the existing data for these reactions are rather poor now and insufficient for such systematical studies. One can hope that in the near future reliable data would be obtained in the experiments at strong current electron accelerators CEBAF and ELSA (see, for example, [48]).

On the other hand, there are the data for coherent reactions

$$p + C \rightarrow [Y^0 K^+] + C \quad (21)$$

obtained in the experiments of the SPHINX Collaboration which might be connected with the Coulomb production mechanism, [47,49].

The feasibility to separate the Coulomb production processes in the coherent proton reactions at  $E_p = 70 \text{ GeV}$  on the carbon target in the measurement with the SPHINX setup has been recently demonstrated in the observation of the Coulomb production of  $\Delta(1232)^+$  isobar with  $I = 3/2$  in the reaction

$$p + C \rightarrow \Delta(1232)^+ + C \quad (22)$$

(see [47]).

## 6 Conclusion

The recent results of the Coulomb production reactions study presented in this talk allow one to obtain the important information on the electromagnetic properties of hadrons and to search for new hadronic structures. We continue the analysis of the data obtained in the SELEX experiment and we hope to improve the precision of these measurements and the number of Primakoff reactions under study.

It is a pleasure for me to express gratitude to my colleagues from the SELEX and SPHINX Collaborations for a tight cooperation in obtaining the main results presented here.

The work is partially supported by RFBR (grant 96-02-16759a).



## References

- [1] Primakoff H., Phys. Rev., 1951, vol. 81, p.119.
- [2] Pomeranchuk I.Ya., Shmushkevich I.M., Nucl. Phys., B, 1961, vol. 23, p. 452.
- [3] Bityukov S.I. et al., Yad.Fiz., 1988, vol. 47, p. 1258.
- [4] Weidenauer, p. et al., Z.Phys. C, 1990, vol. 47, p.353.
- [5] Alde D. et al., Phys.Lett.B, 1994, vol. 340, p. 122.
- [6] Binon F. et al., Yad. Fiz., 1981, vol. 203, p. 327.
- [7] Bityukov, S.I. et al., Phys.Lett.B, 1988, vol. 203, p. 327.
- [8] Landsberg L.G. Fiz. Elem. Chastits At.Yadra, 1990, vol. 21, p. 1054.
- [9] Djhelyadin R.I. et al., Phys.Lett.B, 1980, vol. 94, p. 548.
- [10] Victorov V.A. et al., Yad.Fiz., 1980, vol. 32, p. 1005.
- [11] Landsberg L.G., Phys., Rep., 1985, vol. 128, p. 301.
- [12] Zielinski M., Acta Phys. Polonica B, 1987, vol. 18, p. 455.
- [13] O'Donnell P.J., Rev. Mod. Phys. 1981, vol. 53, p. 673.
- [14] H.Kolanoski, Springer Tracts Mod.Phys., 1984, vol. 105.
- [15] Halpern A. et al., Phys.Rev., 1966, vol. 152, p. 1295.
- [16] Dreitlein J., Primakoff H., Phys.Rev., 1962, vol. 125, p. 591.
- [17] Berlad G. et al., Annals of Phys., 1973, vol. 75, p. 461.
- [18] Fäldt G. et al., Nucl.Phys.B., 1972, vol. 41, p. 125; vol. 43, p. 591.
- [19] Jansen T. et al., Phys.Rev.D, 1983, vol. 27, p. 26.
- [20] Huston J. et al., Phys.Rev.D, 1986, vol. 33, p. 3199.
- [21] Cihangir S. et al., Phys.Lett.B, 1982, vol. 117, p. 119.
- [22] Zeilinski M. et al., Phys.Rev.Lett., 1984, vol. 52, p. 1195.
- [23] Collick B. et al., Phys.Rev.Lett., 1984, vol. 53, p. 2374.
- [24] Berg D. et al., Phys.Lett.B, 1981, vol. 98, p. 119.
- [25] Carismith D. et al., Phys.Rev.Lett., 1986, vol. 56, p. 18.
- [26] Carismith D. et al., Phys.Rev.D, 1986, vol. 36, p. 3199.
- [27] Capraro L. et al., Nucl.Phys.B, 1987, vol.288, p. 659.
- [28] Antipov Yu.M. et al., Phys.Lett.B, vol. 121, p. 445.

- [29] Antipov Yu.M. et al., Phys.Rev.D, vol. 36, p. 21.
- [30] Dydak F., et al., Nucl.Phys.B, 1977, vol. 118, p.1; Delvin T. et al., Phys.Rev.D, vol. 34, p. 1626.
- [31] Peterson P.C. et al. Phys.Rev.Lett., 1986, vol. 57, p. 949.
- [32] Kubarowsky V.P., Report on ICHEP-98, Vancouver, July, 1998.
- [33] Landsberg L.G., Yad.Fiz. (in press)
- [34] Edelstein R. et al., Fermilab Proposal E781, 1987 (revised 1993); Russ J.S., Nisl.Phys, 1995, vol. 585A, p. 39c.
- [35] Smith V.J., Hadron Spectroscopy ("Hadron-97"), Seventh Intern. Conf., Upton, NY, August 1997, (ed, Chung, S-U., Willutzki, H.J.) p. 627.
- [36] Zielinski M. et al., Z. Phys.C, 1983, vol. 16, p. 197.
- [37] Babcock J., Rosner J. L., Phys.Rev., 1976, vol. 14D, p. 1286.
- [38] Ishida S. et al., Phys.Rev, 1989, vol 40D, p. 1497.
- [39] Landsberg L.G., Yad.Fiz., 1996, vol. 59, p. 2161.
- [40] Landsberg L.G., Molchanov V.V., Preprint IHEP 97-42, Protvino, 1997.
- [41] Hogaasen H., Sorba P., Nucl.Phys.B, 1978, vol. 145, p. 119.
- [42] Chan Hoang-Mo, Tsou S.T., Nucl.Phys.B, 1977, vol. 118, p. 413.
- [43] Hirose T. et al., Nuov. Cim.A, 1979, vol. 50A,
- [44] Landsberg L.G., Yad.Fiz. 1994, vol. 57, p. 47; UFN, 1994, vol. 164, p. 1129.
- [45] Zielinski M. et al., Z.Phys.C, 1986, vol. 31, p. 545; vol. 34, p. 255.
- [46] Landsberg L.G., Yad.Fiz., 1990, vol. 52, p. 192; Landsberg L.G., Nucl.Phys.,B (proc.Suppl.), 1991, vol.21, p. 179.
- [47] Vavilov D.V. et al. Yad.Fiz., 1999, vol.62, p.501.
- [48] Shumacher R., Preprint CMU MEG-96-007, Pittsburg, 1996.
- [49] Landsberg L.G., Phys.Rep. (in press).

Experiment	Process under study	Result	Note
LEPTON-F (IHEP) [3] $\omega \rightarrow \pi^+\pi^-\gamma$	$\pi^- + p \rightarrow \omega + n$ ( $P_{\pi^-} = 38$ GeV) $\hookrightarrow \pi^+\pi^-\gamma$	$BR[\omega \rightarrow \pi^+\pi^-\gamma] < 4 \cdot 10^{-3}$ (95% C.L.)	Complicated background conditions due to the main decay channel
ASTERIX (CERN) [4] $\omega \rightarrow \pi^+\pi^-\gamma$	$\bar{p}p \rightarrow \pi^+\pi^-\omega$ (annihilation at rest) $\hookrightarrow \pi^+\pi^-\gamma$	$BR[\omega \rightarrow \pi^+\pi^-\gamma] < 4 \cdot 10^{-3}$ (95% C.L.)	with one lost photon: $\omega \rightarrow \pi^+\pi^-\pi^0 \rightarrow \pi^+\pi^-\gamma(\gamma)$
GAMS-2000 (IHEP-CERN)[5] $\omega \rightarrow \pi^0\pi^0\gamma$	$\pi^- + p \rightarrow [\pi^0\pi^0\gamma] + n$ ( $P_{\pi^-} = 38$ GeV) $\rightarrow \omega + n$ $\hookrightarrow \pi^0\pi^0\gamma$ 40 ± 12 events of the decay $\omega \rightarrow \pi^0\pi^0\gamma$ have been observed	$BR[\omega \rightarrow \pi^0\pi^0\gamma] = (7.2 \pm 2.6) \cdot 10^{-5}$	Favourable background conditions  (no decays $\omega \rightarrow 3\pi^0 \rightarrow \pi^0\pi^0\gamma(\gamma)$ )
GAMS-2000 (IHEP-CERN)[6] $\eta \rightarrow \pi^0\gamma\gamma$	$\pi^- + p \rightarrow \eta + n$ ( $P_{\pi^-} = 38$ GeV) $\hookrightarrow \pi^0\gamma\gamma$ Around 70 events $\eta \rightarrow \pi^0\gamma\gamma$ have been observed	$BR[\eta \rightarrow \pi^0\gamma\gamma] = (9.5 \pm 3.2) \cdot 10^{-4}$	Favourable background conditions (main background is with 2 lost $\gamma$ : $\eta \rightarrow 3\pi^0 \rightarrow \pi^0\gamma(\gamma)\gamma(\gamma)$ )
LEPTON-F (IHEP) [7,8] $D/f_1(1285) \rightarrow \phi\gamma$	$\pi^- + p \rightarrow K^+K^-\gamma + n$ ( $P_{\pi^-} = 32, 5$ GeV) $\rightarrow \phi\gamma + n$ $\hookrightarrow K^+K^-$ 19 ± 5 events of the decay $D/f_1(1285) \rightarrow \phi\gamma$ have been detected	$BR[f_1(1285) \rightarrow \phi\gamma] = (0.9 \pm 0.2 \pm 0.4) \cdot 10^{-3}$	Favourable background conditions (no decays $D/f_1 \rightarrow \phi\pi^0 \rightarrow \varphi\gamma(\gamma)$ )
LEPTON-G (IHEP) [9-11] $\eta \rightarrow \mu^+\mu^-\gamma$ $\eta' \rightarrow \mu^+\mu^-\gamma$	$\pi^- + p \rightarrow [\mu^+\mu^-\gamma] + n$ ( $P_{\pi^-} = 32, 5$ GeV) $\rightarrow \eta; \eta' + n$ $\hookrightarrow \mu^+\mu^-\gamma$ ~ 600 events of the decay $\eta \rightarrow \mu^+\mu^-\gamma$ and 33 ± 7 events of the decay $\eta' \rightarrow \mu^+\mu^-\gamma$ have been observed	$BR[\eta \rightarrow \mu^+\mu^-\gamma] = (3.4 \pm 0.4) \cdot 10^{-4}$ $BR[\eta' \rightarrow \mu^+\mu^-\gamma] = (8.9 \pm 2.4) \cdot 10^{-5}$  Measurements of electromagnetic formfactors of $\eta$ and $\eta'$ mesons	Favourable background conditions (no decays $\eta, \eta' \rightarrow \mu^+\mu^-\pi^0 \rightarrow \mu^+\mu^-\gamma(\gamma)$ )

Table 1: Direct study of rare radiative decays of light mesons.

Table 2: The main features of the Coulomb production processes and the coherent background reactions governed by strong interactions ( $h + (Z, A) \rightarrow a + (Z, A)$ ).

Coulomb production processes	Coherent strong interaction reactions	
	$\omega$ exchange	Pomeron exchange (diffraction)
<p>a) <math>\sigma_{\text{Coulomb}} \propto \ln E_h</math>.</p> <p>b) <math>[d\sigma/dq^2]_{\text{Coulomb}}</math> is in the region of very small <math>q^2</math> (maximum of cross section is at <math>q_0^2 = 2q_{\text{min}}^2 = 2[\frac{M_a^2 - M_h^2}{2E_h}]^2</math>.</p> <p>c) The width of <math>[\frac{d\sigma}{dq^2}]_{\text{Coulomb}}</math> distribution is <math>\Delta \sim 6q_{\text{min}}^2</math>.</p> <p>d) <math>\sigma_{\text{Coulomb}} \propto Z^2</math>.</p> <p>e) In the Gottfrid-Jackson system the <math>t</math>-channel helicity is <math>\lambda = \pm 1</math>, which corresponds to quasi-real virtual photon.</p>	<p>a) <math>\sigma_{\text{strong coh.}} \sim E_h^{-1}</math>, e.g. this process died out at the high energies.</p> <p>b) <math>[d\sigma/dq^2]_{\text{strong coh.}}</math> depends on quantum numbers of particles <math>h</math> and <math>a</math>; in some cases this cross section is reduced in the region of small <math>q^2</math> as <math>[\frac{d\sigma}{dq^2}]_{\text{strong coh.}} \propto (q^2 - q_{\text{min}}^2)</math>.</p> <p>c) <math>\sigma_{\text{strong coh.}} \propto A^{2/3}</math>. As a rule this background is small in the region <math>q^2 \leq 0.003 - 0.01 \text{ GeV}^2</math>.</p>	<p>a) <math>\sigma_{\text{strong}}</math> is practically energy independent (Pomeron exchange).</p> <p>b) <math>[\frac{d\sigma}{dq^2}]_{\text{strong coh.}} \propto \exp[-(q^2 - q_{\text{min}}^2)b]</math> with <math>b \simeq 10 \cdot A^{2/3} \text{ GeV}^{-2}</math>.</p> <p>c) <math>\sigma_{\text{strong coh.}} \propto A^{2/3}</math>.</p> <p>d) <math>t</math>-channel helicity <math>\lambda = 0</math>. Diffractive coherent processes play a main role if they are allowed by quantum numbers:</p> <p>1) <math>h</math> and <math>a</math> have the same flavours;</p> <p>2) <math>h(J^P) \rightarrow a[J^P; (J+1)^{-P}; (J+2)^P]</math> — Gribov-Morrison selection rule.</p>

Experiment	Process under study	Results	Ref.
E272(Fermilab)	$\pi^- + (A, Z) \rightarrow \rho(770)^- + (A, Z)$ ( $P_{\pi^-} = 156; 260\text{GeV}$ ) $\hookrightarrow \pi^+\pi^0$	$\Gamma[\rho(770)^- \rightarrow \pi^- + \gamma] = 71 \pm 7 \text{ keV}$	[20]
	$\pi^+ + (A, Z) \rightarrow \rho(770)^+ + (A, Z)$ ( $P_{\pi^+} = 202\text{GeV}$ ) $\hookrightarrow \pi^+\pi^0$	$\Gamma[\rho(770)^+ \rightarrow \pi^+ + \gamma] = 59.8 \pm 4.0 \text{ keV}$	[19]
	$\rightarrow a_2(1320)^+ + (A, Z)$ $\hookrightarrow \eta\pi^+; K_s^0 K^+$	$\Gamma[a_2(1320)^+ \rightarrow \pi^+ + \gamma] = 295 \pm 60 \text{ keV}$	[21]
	$\rightarrow a_1(1260)^+ + (A, Z)$ $\hookrightarrow 3\pi$	$\Gamma[a_1(1266)^+ \rightarrow \pi^+ + \gamma] = 640 \pm 246 \text{ keV}$	[22]
	$\rightarrow b_1(1235)^+ + (A, Z)$ $\hookrightarrow \omega\pi^+$	$\Gamma[b_1(1235)^+ \rightarrow \pi^+ + \gamma] = 236 \pm 60 \text{ keV}$	[23]
	$K^- + (A, Z) \rightarrow K^*(890)^- + (A, Z)$ ( $P_{K^-} = 156\text{GeV}$ ) $\hookrightarrow K_s^0\pi^-$	$\Gamma[K^*(890)^- \rightarrow K^- + \gamma] = 62 \pm 12 \text{ keV}$	[24]
	Fermilab	$K_L^0 + (A, Z) \rightarrow K^*(896)^0 + (A, Z)$ ( $P_{K^0} = 60 - 200\text{GeV}$ ) $\hookrightarrow K_s^0\pi^0$	$\Gamma[K^*(896)^0 \rightarrow K^0 + \gamma] = 116.5 \pm 9.9 \text{ keV}$
$\rightarrow K^*(1430)^0 + (A, Z)$ $\hookrightarrow K_s^0\pi^0$		$\Gamma[K^*(1420)^0 \rightarrow K^0 + \gamma] < 84 \text{ keV}$ (90% C.L.)	[26]
CERN	$\pi^- + (A, Z) \rightarrow \rho(770)^- + (A, Z)$ ( $P_{\pi^-} = 200\text{GeV}$ ) $\hookrightarrow \pi^-\pi^0$	$\Gamma[\rho(770)^- \rightarrow \pi^- + \gamma] = 81 \pm 4 \pm 4 \text{ keV}$	[27]
SIGMA(IHEP)	$\pi^- + (A, Z) \rightarrow \pi^-\gamma + (A, Z)$ ( $P_{\pi^-} = 40\text{GeV}$ ) Compton $\gamma\pi$ -scattering; measurements of magnetic ( $\beta_\pi$ ) and electric ( $\alpha_\pi$ ) polarizability of pion	$\beta_\pi = (-7.1 \pm 2.8 \pm 1.8) \cdot 10^{-43} \text{ cm}^3$ $\alpha_\pi + \beta_\pi = (1.4 \pm 3.1 \pm 2.5) \cdot 10^{-43} \text{ cm}^3$	[28]
	$\pi^- + (A, Z) \rightarrow \pi^-\pi^0 + (A, Z)$	Study of chiral anomaly $F(\gamma \rightarrow 3\pi) = 12.9 \pm \pm 0.9 \pm 0.5 \text{ GeV}^{-3}$	[29]
CERN	$\Lambda + (A, Z) \rightarrow \Sigma^0 + (A, Z)$ ( $\langle P_\Lambda \rangle = 15 \text{ GeV}$ )	$\Gamma[\Sigma^0 \rightarrow \Lambda + \gamma] = 7.6_{-1.3}^{+2.0} \text{ KeV}$	[30]
Fermilab	$\Lambda + (A, Z) \rightarrow \Sigma^0 + (A, Z)$ ( $\langle P_\Lambda \rangle = 200 \text{ GeV}$ )	$\Gamma[\Sigma^0 \rightarrow \Lambda + \gamma] = 8.6 \pm 0.6 \pm 0.8 \text{ KeV}$	[31]

Table 3: Results of the Primakoff production processes study.

Table 4: Study of the coherent reaction  $\pi^- + (A, Z) \rightarrow (\pi^- \pi^- \pi^+) + (A, Z)$  and the determination of radiative with  $\Gamma[a_2(1320)^- \rightarrow \pi^- + \gamma]$ .

Target	Number of events $\pi^- + (A, Z) \rightarrow$ $\rightarrow (3\pi)^- + (A, Z)$	Number of $a_2(1320)$ events produced in the Coulomb process	$\Gamma[a_2(1320)^- \rightarrow$ $\rightarrow \pi^- + \gamma]$ (keV)	Average value $\Gamma[a_2(1320)^- \rightarrow \pi^- + \gamma]$ (keV)	$\Gamma[a_2(1320)^- \rightarrow \pi^- + \gamma]$ from [21] (keV)	Theoretical predic- tions for $\Gamma[a_2(1320)^- \rightarrow$ $\rightarrow \pi^- + \gamma]$ (keV)
Carbon	2760523	$1587 \pm 480$	$289 \pm 87$	$225 \pm 25(\text{stat.}) \pm$ $\pm 45(\text{syst.}) = 225 \pm 51$	$295 \pm 60$	$348$ [37]
Copper	1997972	$5170 \pm 590$	$248 \pm 27$			$235$ [38]
Lead	549092	$2945 \pm 400$	$198 \pm 27$			

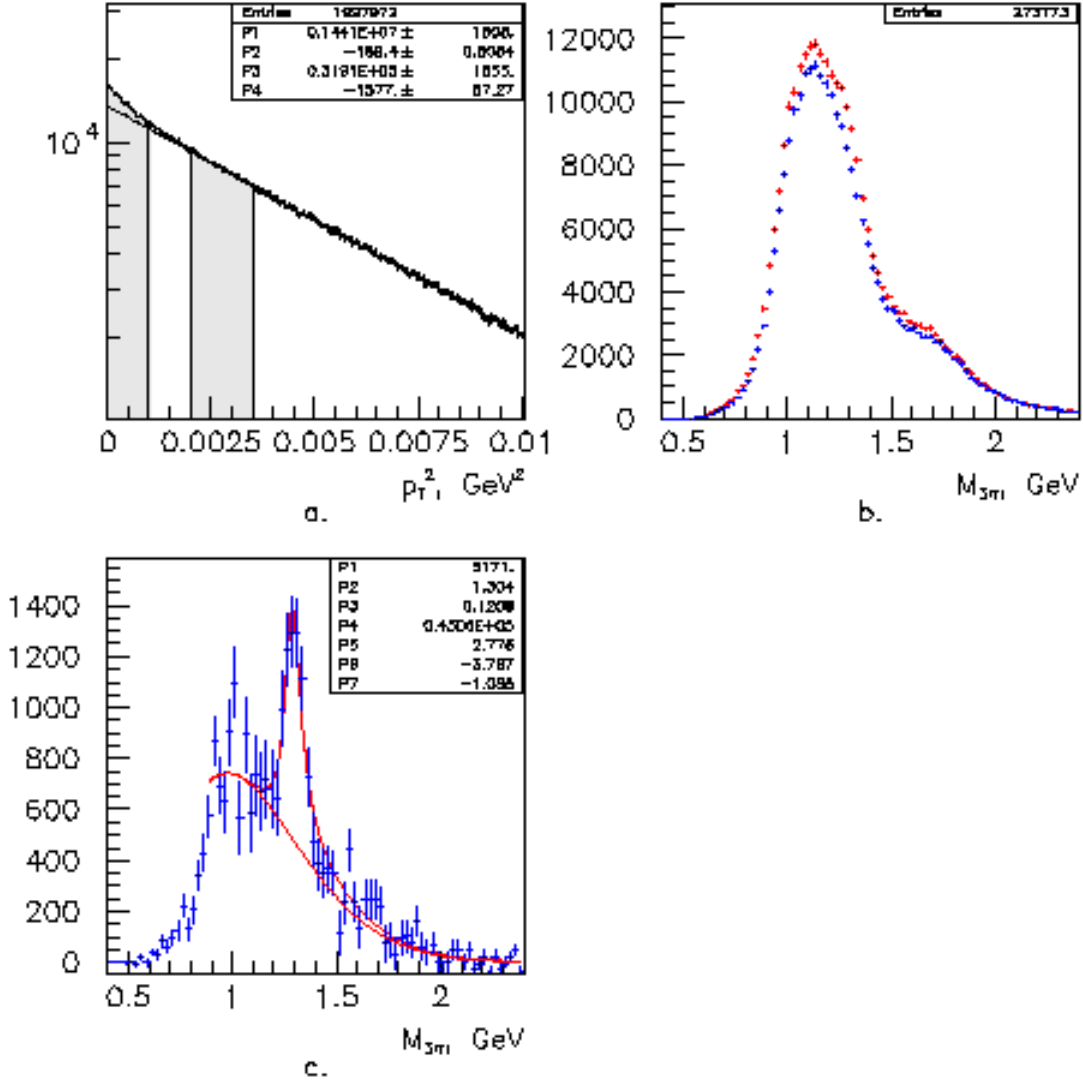


Figure 1: The data for the coherent reaction  $\pi^- + Cu \rightarrow [\pi^- \pi^- \pi^+] + Cu$  at  $E_{\pi^-} = 600$  GeV obtained at the SELEX setup. a)  $dN/dP_T^2$  distribution. The dash line shows the slope for coherent diffraction process caused by the Pomeron exchange. Region 1 ( $P_T^2 < 0.001$  GeV<sup>2</sup>) and region 2 ( $0.0015 < P_T^2 < 0.0035$ ) are used for the Coulomb production separation and for subtraction of the diffractive coherent background. b) Effective mass spectra  $M(3\pi)$  for region 1 (red line) and for region 2 (blue line). c) Effective mass spectrum  $M(3\pi)$  for the Coulomb production process, obtained by subtraction  $M(3\pi)_1 - a \cdot M(3\pi)_2$  after a proper normalization ( $a$  — the normalization factor which was chosen in such a way that the number of diffractive background events in  $N(3\pi)_1$  and  $a \cdot N(3\pi)_2$  were identical).